Research Article

Alfonso Cobo Escamilla, Purificación Bautiste Villanueva*, María Isabel Prieto Barrio, María de las Nieves González García, and Analía Vázquez Bouzón

Effect of basalt fiber length on the behavior of natural hydraulic lime-based mortars

https://doi.org/10.1515/rams-2023-0191 received August 07, 2023; accepted February 24, 2024

Abstract: The number of studies aimed at the characterization of reinforced lime-based mortars for use in the rehabilitation of historic buildings is still very small. This fact contrasts with the growing interest of the industry in these products as substitutes for cement mortars, both for their constructive advantages (compatibility requirements) and their lower cost (economic and environmental). For this reason, this study investigates the effect of basalt fiber length on the physical, mechanical, and durability properties of reinforced natural hydraulic lime mortars and provides criteria for selecting optical blends to meet the various performance requirements for their use as building materials for traditional and contemporary structures. Specimens with 1% volume of basalt fibers and lengths of 6, 12, 18, and 24 mm have been tested. The results in fresh mortar show that increasing the fiber length decreases the consistency and bulk density, as well as increases the air content. Regarding the durability properties of hardened mortar, no direct relationship is observed between fiber length and the decrease in the water absorption coefficient of reinforced mortars. Nor is there a clear relationship between fiber length and the increase in Shore hardness and the decrease in adhesive strength in the reinforced mortars. On the contrary, for small lengths (up to 12 mm), there is a direct

* Corresponding author: Purificación Bautiste Villanueva, Escuela Técnica Superior de Edificación, Universidad Politécnica de Madrid,

Alfonso Cobo Escamilla: Escuela Técnica Superior de Edificación, Universidad Politécnica de Madrid, 28040 Madrid, Spain, e-mail: alfonso.cobo@upm.es

28040 Madrid, Spain, e-mail: p.bautiste@upm.es

María Isabel Prieto Barrio: Escuela Técnica Superior de Edificación, Universidad Politécnica de Madrid, 28040 Madrid, Spain, e-mail: mariaisabel.prieto@upm.es

María de las Nieves González García: Escuela Técnica Superior de Edificación, Universidad Politécnica de Madrid, 28040 Madrid, Spain, e-mail: mariadelasnieves.gonzalez@upm.es

Analía Vázquez Bouzón: Escuela Técnica Superior de Edificación, Universidad Politécnica de Madrid, 28040 Madrid, Spain, e-mail: a.vbouzon@alumnos.upm.es

relationship between fiber length and the increase in other fundamental mechanical properties such as flexural and compressive strength. Based on the results obtained, a predictive model is proposed to determine the amplification factor of flexural and compressive strength as a function of fiber length.

Keywords: mortars, rehabilitation, hydraulic lime, reinforcement, basalt fibers

1 Introduction

The use of lime-based mortars in the construction of buildings and civil works dates back thousands of years. It seems that the Greeks were the first to use pozzolanic additions to lime mortars for the preparation of mortars with hydraulic characteristics, a technology that became known thanks to the later development of the Romans. With the discovery of hydraulic binders during the eighteenth century, aerial limes were gradually replaced by hydraulic limes and, at the beginning of the twentieth century, by Portland cement (PC), a binder with faster hardening and stronger mechanical characteristics [1–6].

It is now known that the use of PC-based mortars for conservation and repair of old buildings with traditional materials present several problems. Some of the main problems are associated with their incompatibility in terms of mechanical, physical, and chemical properties [7-13]. Indeed, PC mortars have a much higher modulus of elasticity and different coefficient of thermal expansion than traditional mortars, which causes stress concentrations when working together [11-14]. Then, PC mortars are less permeable than lime mortars, retaining excess water, which initiate degradation processes. Finally, PC mortars have a high soluble content that promote their migration to the base material, thus accelerating their degradation. Moreover, lime-based mortars are cheaper than PC mortars due to the low price of lime as a binder [12,13]. Lime with hydraulic properties is also interesting for its thermohygrometric properties and its ability to ensure microclimatic conditions (i.e., transpiration, dehumidifying

ability, and insulation) [15]. For all these reasons, in recent years, there has been growing interest in the characterization of both aerial and hydraulic lime-based mortar.

EN 459-1 [16] for building limes defines two product families: (i) air lime which combines and hardens with carbon dioxide present in air, and which is divided into two sub-families, calcium lime (CL) and dolomitic lime; and (ii) lime with hydraulic properties (setting and hardening when mixed with water and/or under water although the reaction with atmospheric carbon dioxide is part of the hardening process) consisting mainly of calcium hydroxide, calcium silicates, and calcium aluminates and organized in three subfamilies: natural hydraulic lime (NHL), formulated lime (FL), and hydraulic lime (HL). NHL is produced by burning of more or less argillaceous or siliceous limestones (including chalk) with reduction to powder by slaking with or without grinding; it does not contain any other additions beyond grinding agents up to 0.1%. FL consists mainly of CL and/or NHL with added hydraulic and/or pozzolanic material. HL is a binder consisting of lime and other materials such as cement, blast furnace slag, fly ash, limestone filler, and other suitable materials.

NHL mortars can provide a good solution for structural restoration of historic buildings due to their similarity to traditional materials, as well as their mechanical efficiency and good workability and durability properties. NHL mortars can be used instead of air-hardening mortars (CL/DL) or lime and pozzolan air-hardening mortars (FL) when early strengths are required [13,17]. Lanas et. al. [13] found that at early ages (up to 28 days) mortars with low lime contents (1:3, 1:4, and 1:5 binder/aggregate volume ratios [B/Ag]) achieved about 80-90% of their maximum value of strength and extend to 50% for 1:1 and 1:2 B/Ag ratios; in this period, the mortars lose the excess water. In addition to faster and higher acquisition of mechanical strength, they have earlier carbonation due to lower lime content, higher ability to harden in moist conditions or underwater, lower dimensional changes, etc. [17]. Medium and long-term durability is also better in NHL lime mortars than FL mortars, mainly due to the presence of aluminate phases in the latter [18]. In addition, the presence of calcium hydroxide provides an important self-healing potential in the event of microcracks appearing, although, in certain climates and conditions, it may be associated with leaching phenomena [17]. On the other hand, the fine porosity (below 0.01 microns of diameter) characteristic of these mortars can favor damage by salt crystallization, and the presence of C-S-H can induce, in conditions of low temperatures and a source of sulfates, the formation of thaumasite leading to cracks or deformations [6,18]. Beyond its use in restoration, NHL mortars have other advantages: it is an eco-efficient material, consumes little energy during its production process, generates few harmful emissions and absorbs carbon dioxide during the carbonation process [18–20].

The introduction of additives (*i.e.*, accelerators, plasticizers, water repellents, and air-entraining agents) and admixtures (*i.e.*, pigments and pozzolana, provided it is added in small quantities and not as a latent binder or fibrous substances) in lime mortars has been driven by the need to improve their physical (workability), mechanical (short and long term strength and ductility), and durability properties; and to reduce defects, such as shrinkage and long setting time [21–32].

One of the most promising lines for improving the properties of NHLs has been the incorporation of fibers at the time of mixing [33–35]. Dafalla et al. [36] have shown the good behavior of lime matrix with polypropylene fibers by finding significant improvements in the tensile strength of clay soils reinforced with polypropylene fibers when small amounts of lime are added as a binder material. This aspect was also proven by Moghal et al. [37,38] in their studies on the improvement of various geotechnical properties in expansive soils. Chan and Bindiganavile [39,40] found improvements in the compressive and flexural strengths of polypropylene fibers reinforced NHL mortars. Bustos et al. [14] did a comparative study on the influence of the addition of glass and carbon fibers on improvements in the mechanical behavior of NHL mortars and found greater increases in flexural strength with carbon fibers. Glass, steel, and polymeric fibers are usually used to control cracking due to plastic and drying shrinkage, increase tensile strength, ductility, toughness, and durability with wide dispersion in the results. There is a broad consensus that NHL mortars reinforced with short fibers homogeneously distributed in the matrix result in materials that behave in a more ductile manner, with a greater capacity to absorb energy before rupture [35,41–43], which is essential for mortars used for repairing historic structures due to the need to accommodate the movements suffered by these constructions as a consequence of thermal variations and creep [22,44,45].

The interest in investigating NHL mortars with basalt fibers stems both from the need to find a more economical alternative to the materials used as reinforcement, and from the obligation to find circular construction materials [46–48]. Basalt fiber is a material with good mechanical properties, including high toughness, high durability, and low production and recycling costs. In addition, it is lightweight, non-combustible, good thermal and acoustic insulator, non-oxidizable, and non-toxic [49–53].

Research on the functionality of basalt fibers in improving the physical, mechanical, and durability

properties of lime mortars is scarce, and is focused on the effect of fiber percentage, and does not yet offer conclusive results. Determining aspects such as fiber geometry in the matrix structure have hardly been dealt with. For this reason, this study presents a set of experimental studies on the influence of basalt fiber size on the improvement of technological properties of NHL mortars for intensive and extensive application as structural repair materials in old and new buildings. The properties of fresh (consistency, dry density, and air content) and hardened mortar (bulk density, capillary water absorption, thermal conductivity, surface hardness, adhesion, flexural strength, and compressive strength) are determined by testing specimens with a fiber volume percentage of 1% and lengths of 6, 12, 18, 24, and 30 mm. The dosage of the reference mortar was previously tested theoretically and experimentally [14,15,17,42,54]. The aim of the article is to provide practical criteria for the choice of the optimum fiber length for each structural requirement.

2 Materials and methods

2.1 Mortars: Materials and mixture

The characteristics of the materials used are detailed below.

Natural hydraulic lime NHL 3.5 from the Saint-Astier company, which meets all the conformity criteria established by the standard EN 459-1 [16].

Silica sand was in accordance with EN 13139 [55]. Figure 1 shows the particle size distribution of aggregate

obtained by sieving according to EN 1015-1 [56]. It is verified that it has a maximum fines content of 3%.

Water for mixing and curing was taken from the drinking water network of the Madrid City Council that complies with the sanitary quality criteria suitable for human consumption according to RD 3/2023, of January 10, and with the technical requirements for mixing and curing concrete and mortar [57,58].

Superplasticizer, water reducer, and accelerator of the mechanical resistance of mortar, were of commercial brand Dynamon NRG 1015 from Mapei that complies with the requirements established by EN 934-1 for concrete and mortar [59]. The superplasticizer is used to facilitate the workability of the mixture during the tests and to accelerate its hardening so that conclusive results can be obtained for the analysis under study at early ages (28 days). The use of this type of additives for the physical-mechanical improvement of the final product is theoretically and experimentally supported [24].

Basalt fibers were obtained from a unidirectional fabric called MAPEWRAP B UNI-AX from Mapei. In order to test the influence of fiber length on the properties of the resulting mortar, the fabric was cut into five different lengths: 6, 12, 18, 24, and 30 mm (Figure 2). Table 1 shows the characteristics of the fiber used.

All specimens have been prepared with a lime:aggregate ratio by weight ($L/A_{\rm w}$) equal to 1:3, commonly used in conservation and rehabilitation works of historical constructions [60,61]. Based on this ratio, the dosage of NHL specimens shown in Table 2 has been determined from the bibliographic update [14,15,17,42] of the experimental research carried out by Bustos [54]. Volume proportions of basalt fiber (1%) were converted in weight to avoid measurement imprecision on mixing process.

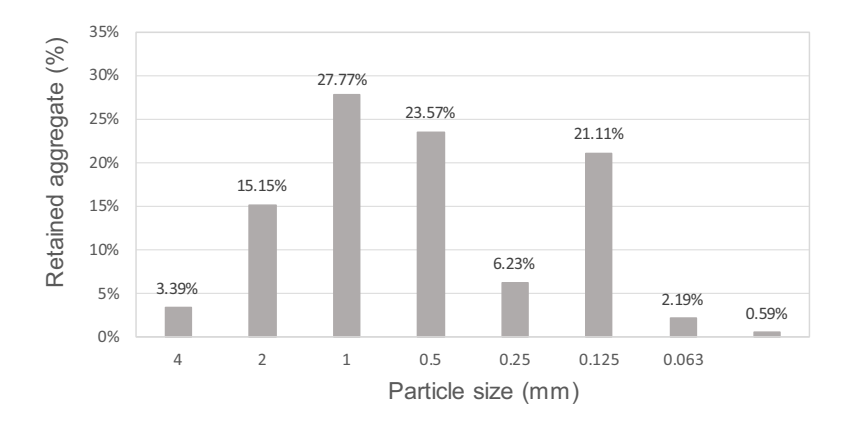


Figure 1: Particle size distribution of aggregate.



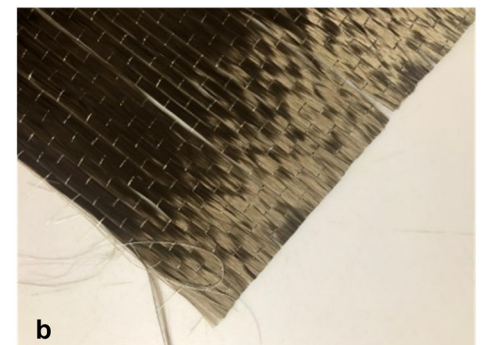


Figure 2: Basalt fibers (a) cut for use and (b) fabric prior to cutting.

Table 1: Properties of basalt fibers

Fiber type	Density (g·cm ⁻³)	Tensile strength (MPa)	Modulus of elasticity (GPa)	Adhesion to concrete (MPa)
MapeWrap B UNI AX	2.75	4,840	89	3

2.2 Testing program

The tests are carried out according to the current European standard [56,62–71] in order to obtain results that can be easily compared with other research already carried out or under development, although Veiga *et al.* [72] pointed out the limitations of some of these tests to adequately characterize the lime mortars used in the conservation of historic buildings. The specified quantities of materials (Table 2) were weighed and mixed in a mechanical mixer. Standard metal molds were filled with the mixture and cured according to the laboratory conditions of each test.

Characterization tests of fresh mortars were carried out in laboratorial controlled standard conditions (temperature $(T) = 20 \pm 3^{\circ}$ C and relative humidity (RH) = 65 ± 5%). Characterization tests of hardened mortars were carried out

at 28 days; the freshly molded mortar samples were placed in a humid chamber for 2 days for initial curing with $T=20\pm 2^{\circ}\text{C}$ and RH = 95 ± 5%; after the first two days, the samples were demolded and continued to be inside humid chamber up to 28 days.

Tests on fresh mortar were performed on a sample of each mix. Tests for hardened mortars were performed on a minimum of three samples of each mix except for dry bulk density and thermal conductivity test for which only one sample of each mortar was used, and water absorption coefficient with two samples per mix; a total of six samples per mix were used in the compression test. Table 3 summarizes the test program for each mix of hardened mortar.

2.2.1 Tests on fresh mortar

The consistency, bulk density, and air content tests were carried out on fresh mortar. These three properties are directly related to the workability of the mortar.

The bulk density of the fresh mortar was obtained according to EN 1015-6 [63], by dividing the weight of fresh mortar filling a container by the interior volume of the container.

Table 2: Composition of the experimental mortars

Id	Lime/sand	Water/solid ^a	Plasticizer	NHL	Sand	Water	Plasticizer	Basalt fiber		
	ratio by weight	ratio by weight	% lime weight	(kg)	(kg)	(m ³)	(kg)	(% mortar volume)	(kg)	Length (mm)
M-RE	1:3	0.182	0.8	490	1,470	358	3.92	0	0	0
M-06	1:3	0.182	0.8	490	1,470	358	3.92	1	21	6
M-12	1:3	0.182	0.8	490	1,470	358	3.92	1	21	12
M-18	1:3	0.182	0.8	490	1,470	358	3.92	1	21	18
M-24	1:3	0.182	0.8	490	1,470	358	3.92	1	21	24
M-30	1:3	0.182	0.8	490	1,470	358	3.92	1	21	30

^aSolid is intended as lime + sand.

Table 3: Test program for each of hardened mortar

		Specimens				
Test	Standard	Number	Shape	Dimensions (mm)		
Dry bulk density	EN 1015-10 [66]	1	Quadrangular prism	160 × 40 × 40		
Water absorption coefficient	EN 1015-18 [67]	2	Quadrangular prism	$80 \times 40 \times 40$		
Thermal conductivity	EN 12664 [68]	1	Quadrangular prism	240 × 240 × 20		
Shore hardness ^a	UNE 102042 [69]	3	Quadrangular prism	160 × 40 × 40		
Adhesive strength	EN 1015-12 [70]	5	Cylinder	50 × 10		
Flexural strength	EN 1015-11 [71]	3	Quadrangular prism	160 × 40 × 40		
Compression strength	EN 1015-11 [71]	6	Quadrangular prism	80 × 40 × 40		

^aFive measurements on each face.

The consistency was determined using the shaking table according to the procedure described by EN 1015-3 [64], introducing the mortar in two layers and compacting each layer with ten blows of the tamper.

The air content test was performed using the pressure method according to the specifications of EN 1015-7 [65].

2.2.2 Physical tests on the hardened mortar

The following physical tests were carried out on the hardened mortar: bulk density, capillary water absorption, and thermal conductivity. These properties are directly related to the durability of the mortar.

The dry bulk density on hardened mortar was determined according to EN 1015-10 [66], by weighing the specimens in an oven until a constant weight was reached and immersing the saturated specimens in water to determine the apparent volume by hydrostatic weighing.

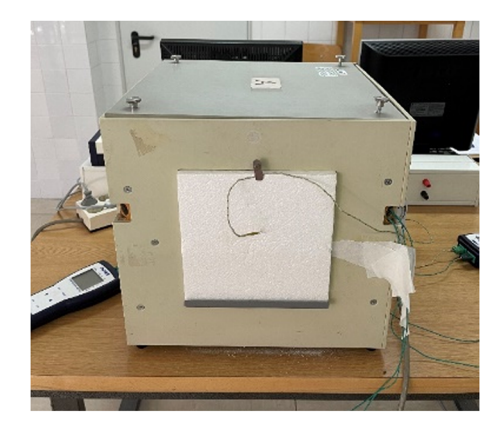
The water absorption coefficient was estimated in accordance with the standard EN 1015-18 [67] although Veiga et al. [72] recommend the use of the standard EN

15801 [73] with some improvements, especially in the case of air lime mortars.

The thermal conductivity was determined according to EN 12664 [68] by the heat flow meter method. For this purpose, specimens were manufactured and cured for 28 days before being placed in an oven at 100°C to obtain a constant weight over time. Then, they were then placed on one side of a closed enclosure at a constant temperature, generated by an internal heat source and a fan, and insulated from the outside with an expanded polystyrene plate. Finally, to determine the conductivity, the temperatures of the interior and exterior air, as well as of the interior and exterior surfaces of the mortar (contact between the plate and the insulation), and of the expanded polystyrene were measured. With these values, the thermal conductivity of the mortar was determined using Eq. (1) (Figure 3).

$$\emptyset = Q/t = \lambda \times \frac{\mathrm{d}T}{\mathrm{d}x} = \lambda \times \frac{T_2 - T_3}{e},$$
 (1)

where $\emptyset = Q/t$ is the heat flow (W·m⁻²), T_2 is the temperature of the interior surface of the mortar (K), T_3 is the temperature of the exterior surface of the mortar in



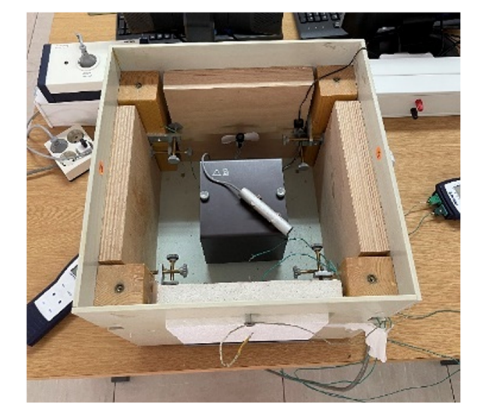


Figure 3: Test enclosure for obtaining thermal conductivity.

contact with the insulating material (K), e is the plate thickness (m), and λ is the thermal conductivity of the material (W·(m⁻¹·K⁻¹)).

2.2.3 Mechanical tests on the hardened mortar

The mechanical tests carried out on hardened concrete are as follows: surface hardness, adhesion, flexural strength, and compressive strength of hardened concrete.

The surface hardness was obtained according to UNE 102042 [69], changing the scale to Shore D hardness. A total of ten measurements are taken from each test tube (five per side).

The adhesion test was performed according to EN 1015-12 [70]. A 10 mm layer of mortar was applied and leveled on a simple hollow brick substrate with dimensions of 400 mm × 200 mm, previously moistened to prevent it from absorbing the water from the mixing. Before hardening, specimens were marked with a truncated coneshaped cylinder of 50 mm diameter. After 28 days of curing, the mortar specimens were bonded to the tensile pads with an epoxy adhesive. Finally, once the adhesive has hardened, tensile force is applied on the tablets until the cylindrical specimen is detached from the brick substrate (Figure 4). The bond strength is calculated using Eq. (2).

$$f_{\rm u} = \frac{F_{\rm u}}{A},\tag{2}$$

where f_u is the adhesive strength (N·mm⁻²), F_u is the breaking load (N), and A is the area of tested surface (mm²).

The fabrication, curing, and testing of the specimens to determine the flexural and compressive strength of the hardened mortar were carried out in accordance with EN 1015-11 [71]. The standard metal molds were filled with the fresh mix in two batches using an IBERTEST

CIB-801 compactor. Testing of the specimens at 28 days was performed with the Ibertest universal press model MIB-60/AM instrumented with displacement transducers. The tests were performed by controlling the displacement at a rate of 0.05 mm·min⁻¹ for the bending test and 0.5 mm·min⁻¹ for the compression test.

The bending tests were performed on prismatic specimens by applying, with the aid of the corresponding adapter, a point load at the center of the span of the upper part of the specimen supported on two points on the lower face 100 mm apart (Figure 9a). The test was performed with a preload of 5 N to avoid premature breakage of the specimen. The value of the flexural strength is obtained with Eq. (3).

$$\sigma_{\rm f} = 1.5 \frac{F \cdot l}{b \cdot d^2},\tag{3}$$

where σ_f is the flexural strength (N·mm⁻²), F is the maximum bending load recorded (N), l is the distance between supports (mm), b is the specimen section width (mm), and d is the specimen section depth (mm).

Compression tests were performed on each of the resulting halves of each specimen tested in bending (Figure 9b) with the same universal press, but changing the adapter used. The compressive strength and strain were obtained from Eqs. (4) and (5).

$$\sigma_{\rm c} = \frac{Q}{S},\tag{4}$$

$$\varepsilon = \frac{L - L_0}{L_0},\tag{5}$$

where σ_c is the compressive strength (N·mm⁻²), Q is the maximum compressive load recorded in the test (N), S is the cross section of the specimen (mm²), ε is the compressive strain (dimensionless), L_0 is the initial length of the specimen (mm), and L is the final length of the specimen (mm).





Figure 4: (a) Adhesive strength test and (b) surface hardness test.

3 Results and discussion

3.1 Tests on fresh mortar

DE GRUYTER

Table 4 shows the results obtained in the tests carried out on fresh mortar. The consistency of the fresh mortar is totally related to the workability of the mortar. The standard EN 1015-3 [64] establishes three types of consistency: dry consistency for values below 140 mm, plastic consistency for values between 140 and 200 mm, and soft or fluid consistency for values above 200 mm. Experience shows that there is a different demand of the consistency based on the use of the mortar in the structure and on the binder [6]. The laboratory workability conditions under which the water quantities of most NHL mortars have been fixed in the ranges of 140 mm [74], 150 mm [17], 134-155 mm [75], 150–155 mm [76], and 140–200 mm [77]; the values obtained for the reference mortar (142 mm) are within these ranges.

There is a clear difference between the consistency of the reference mortar and the consistencies of the mortars with fibers, so that the addition of fibers means a significant reduction in the value of the mortar slump, which is around 110 mm for mortars with fibers compared to 142 mm in the reference mortars. The reason for this decrease is due to the presence of fibers resulting in the formation of a networklike structure that restricts the segregation of the mixture together with the need for a greater amount of binder to envelop all the fibers due to their large specific surface area [78]. As the fiber length increases, the value of the slump decreases, although this decrease is very small.

The bulk density in the fresh state is directly related to the density of the raw material components of the mortar and to the occluded air content. Although the density of basalt fibers (2,750 kg·m⁻³) is higher than that of the reference mortar (2,107 kg·m⁻³), the density of reinforced mortars (variable from 2,041 to 2,099 kg·m⁻³) is lower than that of the reference mortar. This is because the fibers tend to trap air inside the mixture [4,45,79,80].

Table 4: Technological properties of fresh NHL mortars

Id	Consistency (mm)	Bulk density (kg·m ⁻³)	Air content (%)
M-RE	142	2,107	2.4
M-06	113	2,099	2.6
M-12	112	2,093	2.6
M-18	110	2,088	2.8
M-24	109	2,074	2.9
M-30	109	2,041	3.4

The results obtained for the reference mortar (2,107 kg·m⁻³) are similar to those obtained by other authors. Apostolopoulou et al. [17] found an average value of 2,067 kg·m⁻³ for NHL 3.5 and $B/A_{\rm w}$ = 1/3. As the length of the added fiber increases, there is a slight progressive decrease in the value of the mortar density despite the fact that the amount of added fibers is the same in all dosages. This can be explained by a lower compaction of the mortar as the length of fiber added increases.

The air content in fresh mortar is an indicator of the porosity and, therefore, of the long-term behavior of the hardened mortar. The presence of air inside the mortar may be due to air entrapment between the fibers, poor mixing, or inadequate compaction of the mortar. Experimental results show that the occluded air content in reinforced mortars is higher than in reference mortars and that it increases with the increase in the fiber length. The air content amplification factor (relationship between the characteristic values of reinforced and unreinforced mortars) varies from 1.038 for samples with 6 mm fiber length and 1.417 for 30 mm. Microscopic studies show that the inclusion of fibers disrupts the continuity of the mixture [15,39,40].

The joint analysis of the three properties studied for fresh mortar is congruent. Mortars with fibers present lower slump, lower densities, and higher amounts of air content than reference mortars and in addition, the slump and bulk density decrease with fiber length while the occluded air content increases.

Figure 5 shows the relationship between the factors of reduction of consistency and bulk density in relation to the amplification coefficient of the air content with respect to the reference mortar. It is found that there is a good correlation between the increase in air content and the decrease in density ($R^2 = 0.979$), while the relationship with the decrease in slump is poor ($R^2 = 0.381$).

3.2 Physical tests on the hardened mortar

The results of the dry bulk density, water absorption, and thermal conductivity tests performed on the hardened lime mortars are shown in Table 5.

The dry bulk density of the mortars reinforced with basalt fibers is lower than that of the reference mortar and is related to the air content of the mixture. Other authors also found lower bulk density values in basalt fiber reinforced NHL 3.5 mortars ($B/A_{\rm w}$ = 1/3; river sand; 28 dayshumid chamber) [15,42,81]. A relationship between fiber length and dry bulk density value is not appreciated. In any case, for the reinforced mortars, the results obtained 8 — Alfonso Cobo Escamilla et al. DE GRUYTER

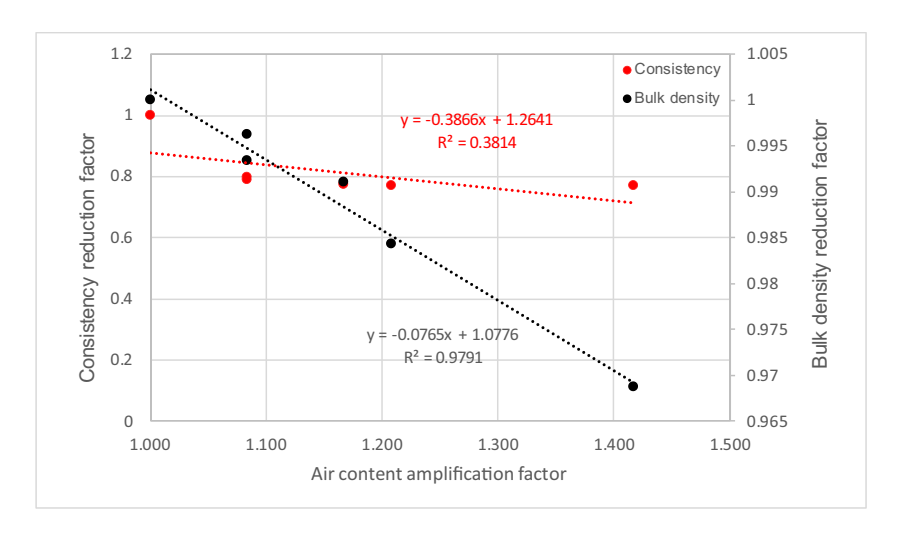


Figure 5: Relationship between air content amplification factor, consistency reduction factor, and bulk density reduction factor.

Table 5: Physical properties of hardened NHL mortars

Id	Dry bulk density (kg·m ⁻³)	Water absorption coefficient (kg/(m²·min ^{0.5}))	Thermal conductivity (W·(m ⁻¹ ·K ⁻¹))
M-RE	2,018	0.81 ± 0.05	0.25
M-06	1,924	0.78 ± 0.04	0.26
M-12	1,933	0.61 ± 0.01	0.27
M-18	1,925	0.65 ± 0.06	0.29
M-24	1,926	0.73 ± 0.04	0.31
M-30	1,935	0.79 ± 0.03	0.36

are very similar, with an average value of $1,929 \, \text{kg} \cdot \text{m}^{-3}$, which is a decrease of 4.4% with respect to the value of the reference mortar.

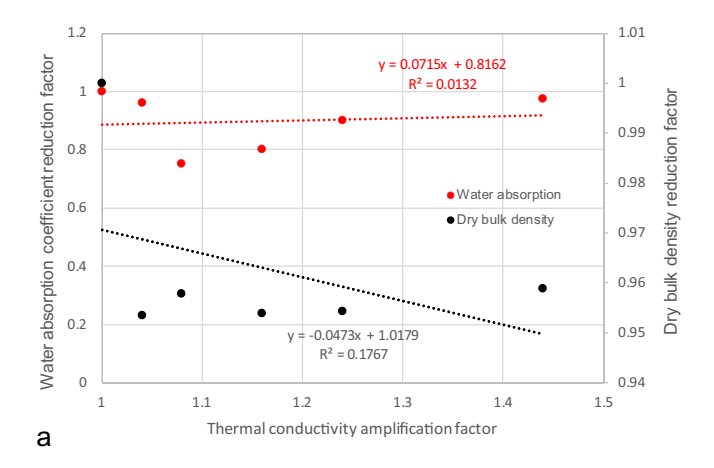
Water absorption coefficient is very important for NHL [82] because it provides valuable information about the size and volume of the open pore network inside the mortar [83]. When mortars are exposed to the action of atmospheric agents, the capillary water absorption coefficient is a determining property for assessing the durability of the mortar, since the inclusion of water in the pore network accelerates the degradation of the material. At the same time, higher water absorption coefficients in NHL mortars are indicative of larger pore sizes and lower risk of degradation by salt crystallization and freeze-thaw [72]. The analysis of Table 5 shows that the water absorption coefficient is higher in the reference mortars than in the reinforced mortars. These results agree with those obtained by other authors with basalt fiber reinforced NHL 3.5 mortars ($B/A_w = 1/3$; river sand; 28-days humid chamber) [4], although it is not possible to establish a trend of relationship with the length of the fibers.

The thermal conductivity is a measure of the mortar's capacity as a thermal insulator. Reinforced mortars have a higher thermal conductivity than reference mortars (Table 5). In addition, an increase in the coefficient can be seen as the length of the added fiber increases. Figure 6 shows the relationship between the amplification or reduction factors with respect to the reference mortar of thermal conductivity vs dry bulk density and water absorption coefficient. The decrease in air content has also been added as a comparison variable. It is observed that there is no relationship between thermal conductivity and water absorption coefficient ($R^2 = 0.0132$), but there is an inverse relationship between thermal conductivity and dry bulk density ($R^2 = 0.1767$), and air content ($R^2 = 0.9823$). These data are contrary to what was expected and could be explained by a variation in the compaction times of the tested specimens, a factor that has a great impact on the values of the thermal conductivity coefficient [84].

3.3 Mechanical tests on the hardened mortar

Table 6 summarizes the mean values and standard deviations of the mechanical tests carried out on the mortars cured at the age of 28 days.

Despite the large dispersion of the results in the hardness tests, it is observed that the lime mortars reinforced with basalt fiber present slightly higher values than those of the reference mortar, although no relationship can be established between the length of the fiber and the hardness of the reinforced mortar. The relationship between the characteristic values of reinforced and unreinforced



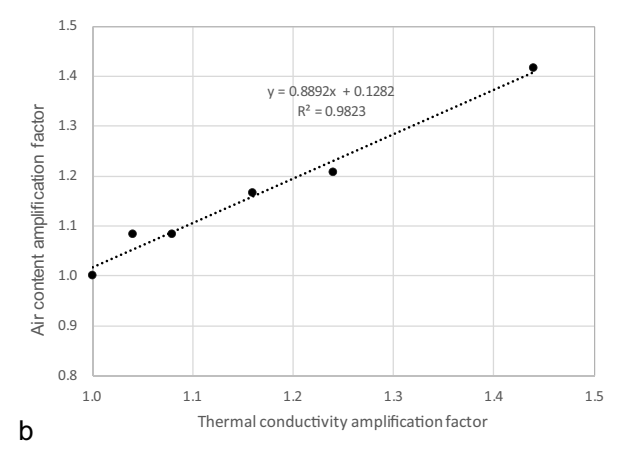


Figure 6: (a) Relationship between thermal conductivity amplification factor, water absorption reduction factor, and dry bulk density reduction factor and (b) relationship between thermal conductivity amplification factor and air content amplification factor.

Table 6: Mechanical properties of hardened NHL mortars

Id	Shore hardness D scale	Adhesive strength (MPa)	Flexural strength (MPa)	Compressive strength (MPa)
M-RE	62.91 ± 1.95	0.25 ± 0.06	0.91 ± 0.02	3.56 ± 0.08
M-06	64.35 ± 1.76	0.20 ± 0.02	1.11 ± 0.05	4.31 ± 0.21
M-12	65.81 ± 1.23	0.20 ± 0.04	1.31 ± 0.03	5.59 ± 0.28
M-18	64.31 ± 0.47	0.14 ± 0.03	1.30 ± 0.17	5.36 ± 0.47
M-24	63.65 ± 0.94	0.19 ± 0.01	1.33 ± 0.08	5.49 ± 0.23
M-30	63.26 ± 1.60	0.16 ± 0.01	1.33 ± 0.03	5.12 ± 0.23

mortars (amplification factors) ranges from 1.01 for NHL-30 mm ln to 1.05 for NHL-12 mm ln. Barbero-Barrera and Flores [85] also found that polypropylene fiber reinforcement of NHL lime pastes (NHL 5; water/blinder = 0.60) slightly increased surface hardness at 90 days when the percentages were small (up to 2%). In contrast, Morón *et al.* [86] obtained slightly lower hardnesses when reinforcing HL mortars with glass, carbon, and basalt fibers (1%)

by volume) (CL-70; cement/aggregate = 1/3 and 1/4, and 28 days-humid chamber).

The adhesive strength of NHLs reinforced with basalt fibers is slightly lower than that of the reference mortar with reduction factors ranging from 0.56 for NHL-18 mm ln to 0.80 for NHL-6 mm ln and NHL-8 mm ln. No clear relationship, however, can be established between increasing fiber length and decreasing adhesive strength in the range of long fibers (>20 mm). Morón *et al.* [86] also found slightly lower results for reinforced HL mortars with cement/aggregate ratios of 1/4 and similar at 1/5 ratios. Zanotti *et al.* [87] found the reverse effect in cement mortars. Spadea *et al.* [43] also confirmed that reinforcement increases the adhesive strength of cement mortars (Figure 7).

Table 7 shows the results of the flexural test, indicating the maximum force resisted by the mortar, the corresponding maximum stress and the displacement reached by the specimen for the maximum stress level, as well as the energy absorbed up to the point corresponding to the maximum stress ($A_{\rm max}$) and the total energy absorbed in





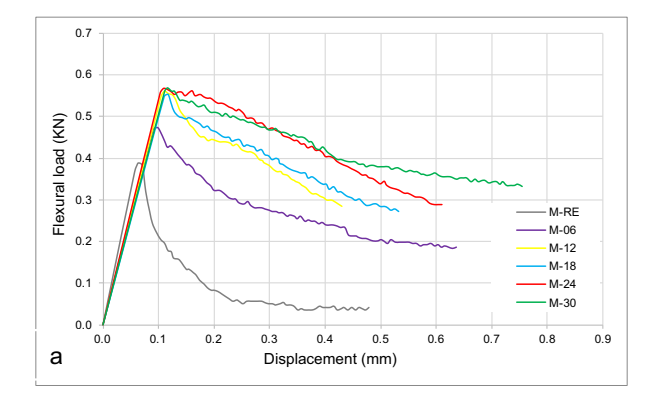


Figure 7: Failure of specimens in adhesive strength test.

10 — Alfonso Cobo Escamilla et al. DE GRUYTER

Table 7: Bending behavior of NHL mortar specimens

Id	Maximum load (KN)	Maximum displacement (mm)	Maximum stress (N·mm ^{−2})	Maximum energy (Nm)	Total energy (Nm)	Ductility
M-RE	0.388 ± 0.007	0.063 ± 0.034	0.909 ± 0.016	0.012 ± 0.007	0.049 ± 0.013	4.02 ± 1.80
M-06	0.475 ± 0.023	0.098 ± 0.072	1.113 ± 0.054	0.023 ± 0.015	0.168 ± 0.006	7.22 ± 1.74
M-12	0.561 ± 0.013	0.110 ± 0.017	1.315 ± 0.030	0.031 ± 0.005	0.207 ± 0.002	6.68 ± 1.18
M-18	0.554 ± 0.073	0.117 ± 0.041	1.298 ± 0.170	0.032 ± 0.016	0.165 ± 0.022	5.16 ± 1.56
M-24	0.566 ± 0.036	0.109 ± 0.043	1.327 ± 0.084	0.031 ± 0.010	0.242 ± 0.016	7.85 ± 1.04
M-30	0.569 ± 0.014	0.116 ± 0.011	1.334 ± 0.034	0.033 ± 0.003	0.306 ± 0.003	9.27 ± 1.03



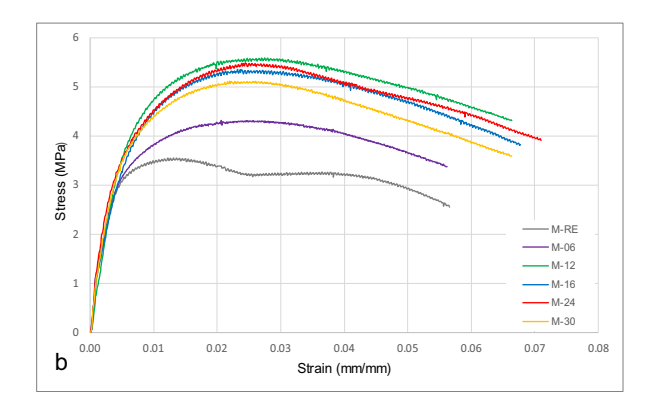


Figure 8: Mechanical behavior of NHL mortars (a) flexural behavior and (b) axial compression behavior.

the test, corresponding to the integral of the load–displacement curve up to the breakage of the specimen ($A_{\rm u}$). The quotient between both values of energy $A_{\rm u}/A_{\rm max}$ is an index of the ductility in terms of energy of each mix.

The average flexural force–displacement curves for each dosage are shown in Figure 8a. The average flexural strength of the control samples was 0.909 N·mm⁻² at 28 days. The maximum strain was reached at an average displacement of 0.063 mm. The specimens show brittle breaks and sudden drops in strength after reaching the maximum load (0.388 N). The behavior is linear up to that point, but the appearance of a first crack quickly triggers failure (Figure 9a).

Reinforcement with basalt fibers increases the flexural strength and ameliorates the sharp decrease in strength after the peak by showing more ductile modes of failure. Specimens with 6 mm fiber lengths have an average flexural strength of 1.11 N·mm⁻², an increase in strength of 22% over the reference mortar. Specimens with longer fiber lengths show very similar peak values, with strengths on the order of 1.30–1.33 N·mm⁻², approximately 45% higher than the reference mortar. The curves show a linear section of similar slope up to the peak load and failure modes that become more ductile as the reinforcement fiber length increases. The drop in strength after the peak is sharper in

the specimens with 6 mm fiber length than in the rest, with very similar failure patterns observed between the 12–18 and 24–30 mm specimens. The energy absorbed until reaching the peak load of the reinforced specimens increases between 90% for specimens with 6 mm length and 160% for the rest of the cases. The total energy increases by 340% on average and the ductility by 80%. In spite of the homogeneity of the failure patterns, there is considerable dispersion in the failure points of the specimens.

Other studies have also shown that reinforcement with basalt fibers increases flexural strength, although with much lower strength amplification factors. Lucolano et al. [15] found almost no variation for specimens with 1% basalt fiber of 4-5 mm length. Similar values were obtained by Asprone et al. [42]. Santarelli et al. [4], on the contrary, provided a strength decrease coefficient of 0.87 for mortars with 3% fibers of 6.35 mm length. Similar losses were obtained by Demircan et al. [81] for specimens reinforced with 1.20% of 6 mm long basalt fiber (flexural strength reduction factor of 0.85). There is unanimity, however, that reinforcement with basalt fiber provides more ductile failure patterns [4,15,42,81]. The disparity in these results, all of them carried out with the same type of lime (NHL 3.5) and aggregate (river sand), at a dosage of $B/A_{\rm w}$ = 1/3, and curing conditions (28 days-humid







Figure 9: Failure of specimens in mechanical tests (a) flexural strength and (b) compressive strength.

chamber), can be explained by the indeterminacy of the technological properties of both materials and by the sensitivity of the interfacial transition zone between the lime matrix and the basalt fiber to factors such as the type and roughness of the fibers, the characteristics and chemical composition, the mineralogical characterizations and particle size of aggregate, and the mixing method. For other types of lime and fiber reinforcement mortars, the results also show a large dispersion: in the study by Rosato et al. [88], a small decrease (NHL mortar reinforced with nanostructured cellulose fibers), in the study by Pachta and Goulas [89], a decrease at 28 days and an increase at 90 days (LP and NHL grouts reinforced with glass and polypropylene fibers), and in the study by Kesikidou and Stefanidou [90], an increase (CL mortar reinforced with jute, coconut, and kelp).

Figure 10 presents the flexural strength amplification factor as a function of basalt fiber length (ratio between the characteristic flexural strength of reinforced and unreinforced mortar). Eq. (6) proposes a prediction model based on the obtained experimental results that shows a good fit. For small fiber lengths, less than 12 mm, the flexural strength increases almost linearly as the fiber length increases; for larger fiber lengths no major increases are observed and the optimum theoretical length would be 23 mm. This effect can be explained because long fiber sizes would produce non-uniform distributions that would affect the continuity of the solid particles, increasing the demand for lime and causing an adverse effect on the workability, porosity, and strength of the mortars.

$$SAF_f = -0.0009x^2 + 0.0418x + 1.0118$$
 $R^2 = 0.9588$. (6)

Table 8 shows the results obtained in the compression tests: maximum stress and strain, ultimate stress and strain, and maximum and ultimate energy densities. The energy density is related to the ductility of the material in compression, and for its calculation, the procedure detailed in the UNE 83508:2006 standard [91] has been carried out,

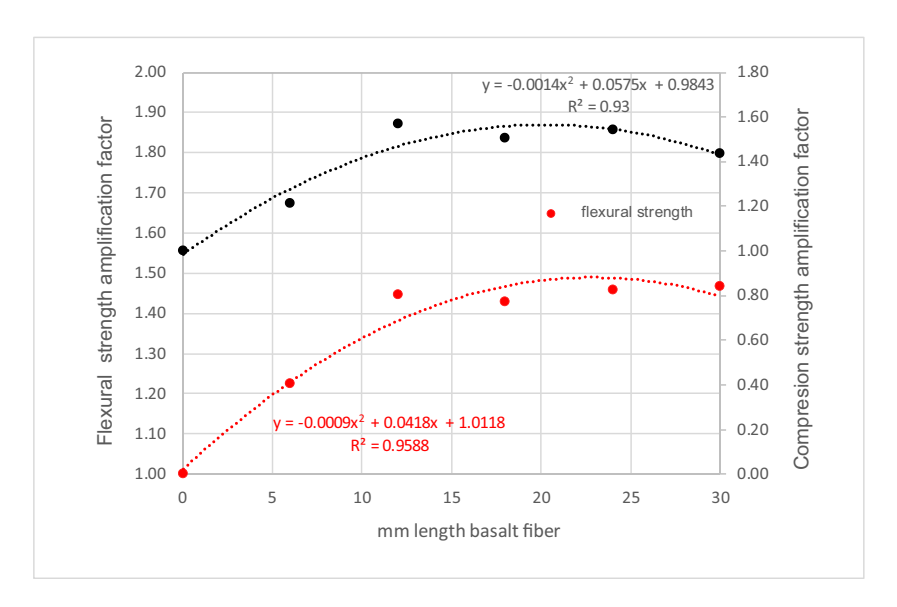


Figure 10: Strength amplification of bending and compression in NHL.

Table 8: Axial compressive behavior of NHL specimens

Id	Maximum stress	Maximum strain	Maximum energy density	Ultimate stress	Ultimate strain	Ultimate energy density	Strain ductility	Energy density ductility
	(N·mm ⁻²)		(N·mm ⁻²)	(N·mm ⁻²)		(N·mm ⁻²)		uucemey
M-RE	3.56 ± 0.08	0.013 ± 0.002	0.037 ± 0.005	2.55 ± 0.24	0.057 ± 0.004	0.176 ± 0.012	4.32 ± 0.48	4.69 ± 0.70
M-06	4.31 ± 0.21	0.021 ± 0.006	0.071 ± 0.020	3.19 ± 0.29	0.060 ± 0.005	0.226 ± 0.023	2.91 ± 0.33	3.16 ± 0.38
M-12	5.59 ± 0.28	0.027 ± 0.003	0.124 ± 0.016	4.31 ± 0.51	0.066 ± 0.004	0.321 ± 0.018	2.42 ± 0.43	2.58 ± 0.49
M-18	5.36 ± 0.47	0.023 ± 0.002	0.096 ± 0.013	3.82 ± 0.54	0.068 ± 0.004	0.309 ± 0.027	2.93 ± 0.25	3.21 ± 0.27
M-24	5.49 ± 0.23	0.024 ± 0.003	0.106 ± 0.017	3.91 ± 0.27	0.071 ± 0.007	0.330 ± 0.046	2.91 ± 0.28	3.12 ± 0.27
M-30	5.12 ± 0.23	0.022 ± 0.005	0.088 ± 0.017	3.59 ± 0.30	0.066 ± 0.011	0.288 ± 0.041	3.03 ± 0.61	3.26 ± 0.70

obtaining the area enclosed by the diagram in the test up to the corresponding stress point. The ratios between the ultimate strain and the strain reached at the point of maximum stress, and the ratio between the ultimate energy density and the maximum energy density have also been obtained. These last two values serve as dimensionless indices to compare the ductility of the six dosages in terms of deformation and in terms of energy.

The average axial compressive stress–strain curves for each dosage are shown in Figure 8b. The compressive strength of the control samples was $3.56~\rm N\cdot mm^{-2}$ at 28 days. The maximum strain was reached at an average displacement of 0.013 mm. The specimens show ductile breaks with smooth drops in the strength after reaching the maximum load ($2.55~\rm N\cdot mm^{-2}$).

Reinforcement with basalt fibers increases the compressive strength and does not improve the strength drop after the peak showing slightly less ductile modes of rupture. Specimens with 6 mm fiber lengths have an average compressive strength of 4.13 N·mm⁻², an increase in strength of 21% over the reference mortar. The specimens with longer fiber lengths show very similar peak values, with strengths in the order of 5.12–5.59 N·mm⁻², approximately 51% higher than the reference mortar. The curves show a similar elastic section and a plastic section that increases with the increase in the fiber length up to the maximum stress, and ductile failure modes that hardly vary with the increase in the fiber length. The equal slope in the elastic section is representative of the fact that the addition of fibers does not substantially alter the modulus of elasticity of NHL mortars, a very important aspect in terms of compatibility between repair mortars and historical mortars. The energy density absorbed until reaching the maximum load of the reinforced specimens increases between 90% for specimens with 6 mm length and 177% for the rest of the cases. The total energy density increases by 28.5% for the 6 mm specimens and between 64 and 87% for the rest of the cases. Consequently, the ductility of the reinforced specimens decreases by 34.7% on average. Homogeneity is observed in the failure patterns and in the points at which the specimens fail.

Other experimental works have determined compressive strength losses in mortars reinforced with basalt fibers. Demircan et al. [81] obtained strength losses of 17% in specimens reinforced with 1.20% of 6 mm long basalt fiber. Deteriorations of 36% were found by Lucolano et al. [15] and Asprone et al. [42] for specimens with 1% basalt fiber of 4-5 mm length. Santarelli et al. [4], on the other hand, also found 40% improvements in compressive strength for mortars with 3% fibers of 6.35 mm length. As mentioned before, the lack of consensus on the influence of synthetic reinforcements on the mechanical properties of NHL mortars is explained by the indeterminacy of the parameters that determine the characteristics of the interfacial transition zone between the lime matrix and the basalt fiber. For other types of lime and fiber reinforcement mortars, the results also show a large dispersion: similar at 28 days and increase at 90 days (LP and NHL grouts reinforced with glass and polypropylene fibers) in the study by Pachta and Goulas [89], and an increase (CL mortar reinforced with jute, coconut, and kelp) in the study by Kesikidou and Stefanidou [90].

Figure 10 presents the compressive strength amplification factor (SAF_c) of reinforced lime mortars as a function of basalt fiber length. Eq. (7) proposes a prediction model based on experimental results, and also shows a good fit. The compressive behavior does not differ substantially from the flexural behavior, and for fiber lengths less than 12 mm, the compressive strength increases almost linearly as the fiber length increases; for longer fiber lengths, no major increases are observed and the optimum theoretical length would be 20 mm.

$$SAF_c = -0.0014x^2 + 0.0575x + 0.9843$$
 $R^2 = 0.93$. (7)

4 Conclusion

Experimental studies have been carried out to analyze the effect of fiber length on the improvement of the workability, physico-mechanical properties, and durability of NHL mortars at early age. The behavior in the fresh and hardened state at 28 days of unreinforced and basalt fiber reinforced mortars has been studied by testing specimens with a fiber volume percentage of 1% and lengths of 6, 12, 18, 24, and 30 mm. The most significant results are as

- There has been a significant effect on the studied properties of the mortar in fresh state: consistency and bulk density decrease and occluded air content increases. In addition, the variation in these properties is related to the fiber length.
- · A decrease in the dry bulk density and in the water absorption coefficient was observed, but no relationship was found between these variations and the length of the fibers. On the contrary, the thermal conductivity increases, there being a relationship between the fiber length and the increase in this property.
- There was an increase in surface hardness and a decrease in adhesion strength. No clear relationship was observed between these variations and fiber length.
- · Reinforcement with basalt fibers increases the flexural strength and ameliorates the sharp decrease in strength after the peak showing more ductile modes of failure. A predictive model is proposed to determine the flexural strength amplification factor as a function of fiber length. For fiber lengths less than 12 mm the flexural strength increases almost linearly as the fiber length increases; for longer fiber lengths, no major increases are observed and the theoretical maximum is of 23 mm. This length should be experimentally tested in future studies.
- Similarly, reinforcement with basalt fibers increases compressive strength, but exhibits slightly less ductile modes of failure as the plastic span before peak stress and the dip slope after reaching peak load increase. The predictive model to determine the compressive strength amplification factor as a function of fiber length presents an optimum value for 20 mm. This length should be experimentally tested in future studies.

In view of these results, it can be concluded that the length of basalt fibers has a strong impact on the consistency, as well as the flexural and compressive strengths and ductility, and to a lesser extent, on the water absorption coefficient and other physical, mechanical, and durability properties studied for reinforced NHL mortars. Although further research would be necessary to contrast

these results, the addition of fibers of lengths in the range of 12-24 mm would improve the mechanical properties of lime mortars for structural repair of old and contemporary buildings with high short-term strength requirements.

Acknowledgments: The authors thank the Building Materials Laboratory of Higher Technical School of Building of the Universidad Politécnica de Madrid for the support of experiments in this research.

Funding information: The authors state no funding involved.

Author contributions: Alfonso Cobo Escamilla: conception, experimental design, and manuscript revision; Purificación Bautiste Villanueva: conception, critical analysis, and composition/edition of manuscript; María Isabel Prieto Barrio: experimental design and test validation; María de la Nieves González Rodríguez: experimental design and test validation; Analía Vázquez Bouzon: carrying out measurements. All authors have accepted responsibility for the entire content of this manuscript and approved its submission.

Conflict of interest: The authors state no conflict of interest.

References

- [1] Sağın, E. U., H. E. Duran, and H. Böke. Lime mortar technology in ancient eastern Roman provinces. Journal of Archaeological Science: Reports, Vol. 39, 2021, id. 103132.
- Cowper, A. Lime and Lime Mortars (first published in 1927 for the Building Research Station by HM Stationery Office, London), 1st. ed., Donhead Publishing Ltd, Dorset, 1998.
- [3] Moropoulou, A., A. Bakolas, and K. Bisbikou. Investigation of the technology of historic mortars. Journal of Cultural Heritage, Vol. 1, 2000, pp. 45-58.
- Santarelli, M. L., F. Sbardella, M. Zuena, J. Tirillò, and F. Sarasini. [4] Basalt fiber reinforced natural hydraulic lime mortars: A potential bio-based material for restoration. Materials & Design, Vol. 63, 2014, pp. 398-406.
- Adam, J. P. Roman building materials and techniques, 1st. ed., [5] Routledge, London and New York, 1995.
- [6] Groot, C., R. Veiga, I. Papayianni, R. Van Hees, M. Secco, J. I. Alvarez, et al. RILEM TC 277-LHS report: lime-based mortars for restoration-a review on long-term durability aspects and experience from practice. Materials and Structures, Vol. 55, 2022, id. 245.
- Goldsworthy, H. and Z. Min. Mortar studies towards the replication of Roman concrete. Archaeometry, Vol. 51, No. 6, 2009, pp. 932-946.
- Diaz, J., R. Ševcík, P. Mácová, B. Menéndez, D. Frankeová, and [8] Z. Slížková. Impact of nanosilica on lime restoration mortars properties. Journal of Cultural Heritage, Vol. 55, 2022, pp. 210-222.
- Bochen, J. and M. Labus. Study on physical and chemical properties of external lime-sand plasters of some historical buildings. Construction and Building Materials, Vol. 45, 2013, pp. 11-19.

- [10] Matias, G., P. Faria, and I. Torres. Lime mortars with heat treated clays and ceramic waste: a review. *Construction and Building Materials*, Vol. 73, 2014, pp. 125–136.
- [11] Ruegenberg, F., M. Schidlowski, T. Bader, and A. Diekamp. NHL-based mortars in restoration: Frost-thaw and salt resistance testing methods towards a field related application. *Case Studies in Construction Materials*, Vol. 14, 2021, id. e00531.
- [12] Lanas, J. and J. I. Álvarez-Galindo. Masonry repair lime-based mortars: factors affecting the mechanical behavior. *Cement and Concrete Research*, Vol. 33, 2003, pp. 1867–1876.
- [13] Lanas, J., J. L. Pérez Bernal, M. A. Bello, and J. L. Álvarez Galindo. Mechanical properties of natural hydraulic lime-based mortars. Cement and Concrete Research, Vol. 34, 2004, pp. 2191–2201.
- [14] Bustos, A., E. Moreno, F. González-Yunta, and A. Cobo. Influence of addition of fibers on properties of the hydraulic lime mortars. *Dyna*, Vol. 94, 2018, pp. 228–232.
- [15] Lucolano, F., B. Liguori, and C. Colella. Fibre-reinforced lime-based mortars: A possible resource for ancient masonry restoration. *Construction and Building Materials*, Vol. 38, 2013, pp. 785–789.
- [16] EN 459-1: 2011. Building lime Part 1: definitions, specifications and conformity criteria.
- [17] Apostolopoulou, M., A. Bakolas, and M. Kotsainas. Mechanical and physical performance of natural hydraulic lime mortars. Construction and Building Materials, Vol. 290, 2021, id. 123272.
- [18] Álvarez, J. I., R. Veiga, S. Martínez-Ramírez, M. Secco, P. Faria, P. N. Maravelaki, et al. RILEM TC 277-LHS report: a review on the mechanisms of setting and hardening of lime-based binding systems. *Materials and Structures*, Vol. 54, 2021, id. 63.
- [19] Jayasingh, S. and J. Baby. Influence of organic addition on strength and durability of lime mortar prepared with clay aggregate. *Materials Today*, Vol. 64, 2022, pp. 1006–1013.
- [20] Quattrociocchi, G., M. Valente, F. Sarasini, J. Tirillò, and M. L. Santarelli. Basalt fiber as reinforcement for lime-based mortars. In: Proceedings of the 1st International Conference on Bio-based Building Materials; 2015 June 22-24, RILEM Publications, Clermont-Ferrand, France, 2015, pp. 57–62.
- [21] Di Bella, G., V. Fiore, G. Galtieri, C. Borsellino, and A. Valenza. Effects of natural fibers reinforcement in lime plasters (kenaf and sisal vs polypropylene). Construction and Building Materials, Vol. 58, 2014, pp. 159–165.
- [22] Van Balen, K., I. Papayianni, R. Van Hees, L. Binda, and A. Waldum. Introduction to requirements for and functions and properties of repair mortars. *Materials and Structures*, Vol. 38, 2005, pp. 781–785.
- [23] Stefanidou, M., V. Kamperidou, A. Konstantinidis, P. Koltsou, and S. Papadopoulos. Use of Posidonia oceanica fibres in lime mortars. Construction and Building Materials, Vol. 298, 2021, id. 123881.
- [24] Maravelaki, P. N., K. Kapetanaki, I. Papayianni, I. Ioannou, P. Faria, J. Alvarez, et al. RILEM TC 277-LHS report: additives and admixtures for modern lime-based mortars. *Materials and Structures*, Vol. 56, 2023, id. 106.
- [25] Grilo, J., P. Faria, R. Veiga, A. Santos Silva, V. Silva, and A. Velosa. New natural hydraulic lime mortars – Physical and microstructural properties in different curing conditions. *Construction and Building Materials*, Vol. 54, 2014, pp. 378–384.
- [26] Sepulcre, A. Influencia de las adiciones puzolánicas en los morteros de restauración de fábricas de interés histórico-artístico. PhD tesis. Universidad Politécnica de Madrid, Madrid, 2005.
- [27] González, M. and L. De Villanueva. Morteros hidráulicos de cal y chamota. *Mater de Construcción*, Vol. 266, 2002, pp. 65–76.

- [28] Benchiheub, D., C. Amouri, H. Houari, and M. Belachia. Effect of natural pozzolana and polypropylene fibers on the performance of lime mortar for old buildings restoration. *Journal of Adhesion Science* and Technology, Vol. 32, No. 12, 2018, pp. 1324–1340.
- [29] Pujadas, P. Caracterización y diseño del hormigón reforzado con fibras plásticas. PhD tesis. Universidad Politécnica de Cataluña, Barcelona, 2013.
- [30] Papayianni, I. and V. Pachta. Experimental study on the performance of lime-based grouts used in consolidating Historic Masonries. *Materials and Structures*, Vol. 48, 2015, pp. 2111–2121.
- [31] Papayianni, I., M. Stefanidou, and V. Pachta. Grouts for injection of historical masonries: influence of the binding system and other additions on the properties of the matrix. In: 2nd Conference on Historic Mortars - HMC 2010 and RILEM TC 203-RHM final workshop, 2010 September 22–24; Prague, Czech Republic. RILEM Publications SARL; 2010, pp. 1123–1133.
- [32] Baltazar, L. G., F. M. A. Henriques, F. Jorne, and M. T. Cidade. Combined effect of superplasticizer, silica fume and temperature in the performance of natural hydraulic lime grouts. *Construction and Building Materials*, Vol. 50, 2014, pp. 584–597.
- [33] Badagliacco, D., B. Megna, and A. Valenza. Induced modification of flexural toughness of natural hydraulic lime based mortars by addition of giant reed fibers. Case Studies in Construction Materials, Vol. 13, 2020, id. e00425.
- [34] Mallat, A. and A. Alliche. Mechanical investigation of two fiberreinforced repair mortars and the repaired system. *Construction and Building Materials*, Vol. 25, 2011, pp. 1587–1595.
- [35] Izaguirre, A., J. Lanas, and J. I. Alvarez. Effect of a polypropylene fiber on the behavior of aerial lime-based mortars. *Construction and Building Materials*, Vol. 25, 2011, pp. 992–1000.
- [36] Dafalla, M. A., A. A. B. Moghal, and A. K. Al-Obaid. Enhancing tensile strength in clays using polypropylene fibers. *GEOMATE Journal*, Vol. 12, No. 29, 2017, pp. 33–37.
- [37] Moghal, A. A. B., C. S. Bhaskar, B. Chittoori, M. Basha, and A. M. Al-Mahbashi. Effect of polypropylene fibre reinforcement on the consolidation, swell and shrinkage behavior of lime-blended expansive soil. *International Journal of Geotechnical Engineering*, Vol. 12, No. 5, 2018, pp. 462–471.
- [38] Rehman, A. U. and A. A. B. Moghal. The influence and optimization of treatment strategy in enhancing semiarid soil geotechnical properties. *Arabian Journal for Science and Engineering*, Vol. 43, 2018, pp. 5129–5141.
- [39] Chan, R. and V. Bindiganavile. Toughness of fibre reinforced hydraulic lime mortar. Part-1: Quasi-static response. *Materials and Structures*, Vol. 43, 2010, pp. 1435–1444.
- [40] Chan, R. and V. Bindiganavile. Toughness of fibre reinforced hydraulic lime mortar. Part-2: Dynamic response. *Materials and Structures*, Vol. 43, 2010, pp. 1445–1455.
- [41] Asprone, D., F. Lucolano, E. Cadoni, and A. Prota. Analysis of the strain-rate behavior of a basalt fiber reinforced mortar. *Applied Mechanics and Materials*, Vol. 82, 2011, pp. 196–201.
- [42] Asprone, D., E. Cadoni, F. Lucolano, and A. Prota. Analysis of the strain-rate behavior of a basalt fiber reinforced natural hydraulic mortar. *Cement and Concrete Composites*, Vol. 53, 2014, pp. 52–58.
- [43] Spadea, S., I. Farina, A. Carrafiello, and F. Fraternali. Recycled nylon fibers as cement mortar reinforcement. *Construction and Building Materials*, Vol. 80, 2015, pp. 200–209.
- [44] Nez erka, V., J. Antoš, J. Litoš, and J. Zeman. An integrated experimental-numerical study of the performance of lime-based mortars

- in masonry piers under eccentric loading. Construction and Building Materials, Vol. 114, 2016, pp. 913-924.
- [45] De la Rosa Ortiz, G. A. Comportamiento mecánico de hormigones a base de mortero de cal y barras de fibra de vidrio para su implementación en rehabilitaciones del patrimonio edificado. MSc thesis. Universidad Politécnica de Cataluña, Barcelona, 2016.
- [46] Dhand, V., G. Mittal, K. Y. Rhee, S. J. Park, and D. Hui. A short review on basalt fiber reinforced polymer composites. Composites Part B: Engineering, Vol. 73, 2015, pp. 166-180.
- [47] Deak, T. and T. Czigany. Chemical composition and mechanical properties of basalt and glass fibers: a comparison. Textile Research Journal, Vol. 79, 2009, pp. 645-651.
- [48] Gregor-Svetec, D. and F. Sluga. High modulus polypropylene fibers. I. Mechanical properties. Journal of Applied Polymer Science, Vol. 98, 2005, pp. 1-8.
- [49] Telosworld. Minerales estratégicos. Fibra continua de basalto, 2020. https://telosworld.com/fibra-continua-de-basalto/.
- [50] Schiavon, M. A., S. U. A. Redondo, and I. V. P. Yoshida. Thermal and morphological characterization of basalt continuous fibers. Cerâmica, Vol. 53, No. 326, 2007, pp. 212-217.
- [51] Wei, B., H. Cao, and S. Song. Tensile behavior contrast of basalt and glass fibers after chemical treatment. Materials & Design, Vol. 31, 2010, pp. 4244-4250.
- [52] Wei, B., H. Cao, and S. Song. Degradation of basalt fibre and glass fibre/epoxy resin composites in seawater. Corrosion Science, Vol. 53, 2011, pp. 426-431.
- [53] Quattrociocchi, G., M. Able, J. Tirillo, F. Sarasini, M. Valente, and M. L. Santarelli. Basalt fibers as a sustainable reinforcement for cement based mortars: preliminary study, materials characterization VII 109. WIT Transactions on Engineering Sciences, Vol. 90, 2015, pp. 109-120.
- [54] Bustos, A. Morteros con propiedades mejoradas de ductilidad por adición de fibras de vidrio, carbono y basalto. PhD tesis. Universidad Politécnica de Madrid, Madrid, 2018.
- [55] EN 13139: 2003. Aggregates for mortar.
- [56] EN 1015-1:1999/A1:2007. Methods of test for mortar for masonry -Part 1: Determination of particle size distribution (by sieve analysis).
- [57] Real Decreto 3/2023, de 10 de enero, por el que se establecen los criterios técnico-sanitarios de la calidad del agua de consumo, su control y suministro.
- [58] Real Decreto 470/2021, de 29 de junio, por el que se aprueba el Código Estructural.
- [59] EN 934-1:2009. Admixtures for concrete, mortar and grout Part 1: Common requirements.
- [60] Drdácký, M., D. Mašín, M. Mekonone, and Z. Slížková. Compression tests on non-standard historic mortar specimen. Proceedings of the 1st Historical Mortars Conference HMC08, Lisbon, Portugal, 2008.
- [61] Drdácký, M., Z. Slížková, and A. Zeman. Analysis and restoration of an exterior plaster floor of the 19th century. In: Heritage, Weathering and Conservation, Taylor & Francis Group, London, 2006, pp. 961-968.
- [62] EN 1015-2:1999/A1:2007. Methods of test for mortar for masonry -Part 2: Bulk sampling of mortars and preparation of test mortars.
- [63] EN 1015-6:1999. Methods of test for mortar for masonry Part 6: Determination of bulk density of fresh mortar.
- [64] EN 1015-3: 2000. Methods of test for mortar for masonry -Determination of consistence of fresh mortar (by flow table).
- [65] EN 1015-7:1999. Methods of test for mortar for masonry Part 7: Determination of air content of fresh mortar.
- [66] EN 1015-10:2000. Methods of test for mortar for masonry Part 10: Determination of dry bulk density of hardened mortar.

- [67] EN 1015-18:2003. Methods of test for mortar for masonry Part 18: Determination of water absorption coefficient due to capillary action of hardened mortar.
- [68] EN 12664:2002. Thermal performance of building materials and products. Determination of thermal resistance by means of guarded hot plate and heat flow meter methods. Dry and moist products of medium and low thermal resistance.
- [69] UNE 102042:2014. Gypsum plasters. Other test methods. AENOR ed. Madrid-España, 2014.
- [70] EN 1015-12:2016. Methods of test for mortar for masonry Part 12: Determination of adhesive strength of hardened rendering and plastering mortars on substrates.
- EN 1015-11:2020. Methods of test for mortar for masonry Part 11: Determination of flexural and compressive strength of hardened
- [72] Veiga, R., P. Faria, R. Van Hees, M. Stefanidou, P. N. Maravelaki, I. Papayianni, et al. RILEM TC 277-LHS report: properties of limebased renders and plasters - discussion of current test methods and proposals for improvement. Materials and Structures, Vol. 56, 2023, id. 70.
- [73] EN 15801:2010. Conservation of cultural property Test methods -Determination of water absorption by capillarity.
- Paiva, H., V. B. Ferreira, and J. A. Labrincha. Effects of a water retaining agent on the rheological behavior of a single-coat render mortar. Cement and Concrete Research, Vol. 36, 2006, pp. 1257-1262.
- Maravelaki-Kalaitzaki, P., A. Bakoas, I. Karatasios, and V. Kilikoglou. [75] Hydraulic lime mortars for the restoration of historic masonry in Crete. Cement and Concrete Research, Vol. 35, No. 8, 2005, pp. 1577-1586.
- [76] Garijo, L., X. Zhang, G. Ruiz, J. J. Ortega, and Z. Wu. The effects of dosage and production process on the mechanical and physical properties of natural hydraulic lime mortars. Construction and Building Materials, Vol. 169, 2018, pp. 325-334.
- [77] Jornet, A., C. Mosca, G. Cavallo, and G. Corredig. Comparison between traditional, lime based, and industrial, dry mortars. In: Proceedings of the 2nd Historic Mortars Conference HMC2010 and RILEM TC 203-RHM Final Workshop;2010 Sep 22-24; Prague, Czech Republic, RILEM Publications, 2010, pp. 631-644.
- [78] Chen, B., K. Wu, and W. Yao. Conductivity of carbon fiber reinforced cement-based composites. Cement and Concrete Composites, Vol. 26, No. 4, 2004, pp. 291-297.
- [79] Chung, D. D. Electrically conductive cement-based materials. Advances in Cement Research, Vol. 16, No. 4, 2004, pp. 167-176.
- Graham, R. K., B. Huang, X. Shu, and E. G. Burdette. Laboratory evaluation of tensile strength and energy absorbing properties of cement mortar reinforced with micro-and meso-sized carbon fibers. Construction and Building Materials, Vol. 44, 2013, pp. 751-756.
- [81] Demircan, R. K., B. A. Tayeh, D. N. Celik, G. Kaplan, and D. E. Tobbala. The effect of animal and synthetic fibers on the physicomechanical durability and microstructure properties of natural hydraulic lime-based mortars. Materials Today Communications, Vol. 35, 2023, id. 106041.
- [82] Arandigoyen, M., J. L. P. Bernal, M. A. B. López, and J. L. Álvarez. Lime-pastes with different kneading water: pore structure and capillary porosity. Applied Surface Science, Vol. 252, 2005,
- [83] Barbero-Barrera, M. M., L. S. Gómez-Villalba, D. Ergenc, A. Sierra-Fernández, and R. Fort, Influence of curing conditions on the mechanical and hydric performance of air-lime mortars with nano-

- $Ca(OH)_2$ and nano-SiO₂ additions. *Cement and Concrete Composites*, Vol. 132, 2022, id. 104631.
- [84] Barbero-Barrera, M. M., A. García-Santos, and F. J. Neila-González. Thermal conductivity of lime mortars and calcined diatoms. Parameters influencing their performance and comparison with the traditional lime and mortars containing crushed marble used as renders. *Energy and Buildings*, Vol. 76, 2014, pp. 422–428.
- [85] Barbero-Barrera, M. M. and N. Flores. The effect of polypropylene fibers on graphite-natural hydraulic lime pastes. *Construction and Building Materials*, Vol. 184, 2018, pp. 591–601.
- [86] Morón, A., D. Ferrández, P. Saiz, E. Atanes-Sánchez, and C. Morón. Study of the properties of lime and cement mortars made from recycled ceramic aggregate and reinforced with fibers. *Journal of Building Engineering*, Vol. 35, 2021, id. 102097.
- [87] Zanotti, C., N. Banthia, and G. Plizzari. A study of some factors affecting bond in cementitious fiber reinforced repairs. *Cement and Concrete Research*, Vol. 63, 2014, pp. 117–126.
- [88] Rosato, L., M. Stefanidou, G. Milazzo, F. Fernandez, P. Livreri, N. Muratore, et al. Study and evaluation of nano-structured cellulose fibers as additive for restoration of historical mortars and plasters. *Materials Today: Proceedings*, Vol. 4, No. 7, 2017, pp. 6954–6965.
- [89] Pachta, V. and D. Goulas. Fresh and hardened state properties of fiber reinforced lime-based grouts. *Construction and Building Materials*, Vol. 261, 2020, id. 119818.
- [90] Kesikidou, F. and M. Stefanidou. Natural fiber-reinforced mortars. *Journal of Building Engineering*, Vol. 25, 2019, id. 100786.
- [91] UNE 83508:2004. Concrete with fibers. Determination of the index of tenacity in compression. AENOR ed. Madrid-España, 2004.